

Preplanned Studies

Epidemiological Transition and Spatial Expansion of Mountain-Type Zoonotic Visceral Leishmaniasis — China, 2010–2024

Lulu Huang¹; Yanfeng Gong²; Zhengbin Zhou¹; Jingshu Liu¹; Peijun Zhang³; Shizhu Li^{1#}

Summary

What is already known about this topic?

Mountain-type zoonotic visceral leishmaniasis (MT-ZVL) remains endemic in China and has re-emerged in recent years, with its geographic distribution demonstrating signs of progressive expansion.

What is added by this report?

Drawing on 15 years of national surveillance data, this study demonstrates a clear resurgence after 2015, a shift in high-risk populations from scattered children to farmers and older adults, and eastward and northward expansion of transmission risk areas.

What are the implications for public health practice?

These findings provide evidence that control strategies should prioritize interventions targeting farmers and elderly-focused interventions, strengthen surveillance in newly affected counties, and implement geographically targeted vector and reservoir control measures.

during 2015–2024, with projections indicating continued growth by 2030 without strengthened control.

Conclusions: MT-ZVL in China shows expanding risk areas and changing occupational patterns, highlighting the need for strengthened surveillance and targeted control interventions in the regions.

Visceral leishmaniasis (VL), also known as kala-azar, is a neglected tropical disease that is fatal in over 95% of untreated cases (1). Mountain-type zoonotic visceral leishmaniasis (MT-ZVL) represents the predominant form of VL in China, accounting for more than 95% of reported cases. The disease is transmitted by *P. chinensis*, with dogs and certain wild animals serving as the primary reservoir hosts (2). Following large-scale control efforts initiated in the 1950s, MT-ZVL incidence declined substantially and was largely controlled by the 1960s. However, re-emergence and geographic expansion of MT-ZVL have been observed across multiple provinces in northern and central China over the past decade, raising concerns about the sustainability of previous control achievements (3–5). Recent surveillance data from China's National Notifiable Diseases Reporting System (NNDRS) reveal shifts in the demographic and occupational profiles of MT-ZVL cases, with increasing involvement of farmers and older adults and a corresponding decline among young children. Concurrently, indigenous cases have been reported in an increasing number of counties, including areas previously not considered endemic, suggesting gradual expansion of transmission zones. These evolving patterns challenge traditional control approaches that focus primarily on historically endemic foci. This study characterizes the demographic features, occupational distribution, temporal trends, and geographic expansion of MT-ZVL transmission in China, providing evidence to inform targeted and adaptive public health interventions.

ABSTRACT

Introduction: Mountain-type zoonotic visceral leishmaniasis (MT-ZVL) has re-emerged in China with shifting demographic patterns and expanding geographical distribution. This study aimed to characterize its epidemiological and spatial-temporal dynamics to guide targeted control strategies.

Methods: Case data from 2010–2024 were analyzed using χ^2 tests and proportional analyses. Temporal trends were assessed by Joinpoint regression, projections by autoregressive integrated moving average (ARIMA) models, spatial clustering and directional tendency by *Moran's I* and Standard Deviational Ellipse (SDE) analyses.

Results: A total of 2,260 cases were reported, showing a bimodal age distribution (<5 years and 60–75 years) with marked male predominance and a shifting occupational risk toward adults. Affected counties expanded from 19 to 69 and after a decline in 2010–2015, incidence increased and spread eastward

MT-ZVL surveillance data were obtained from the NNDRS from January 1, 2010, to December 31, 2024, covering 7 endemic provincial-level administrative divisions (PLADs): Beijing Municipality and 6 provinces (Shanxi, Shaanxi, Gansu, Sichuan, Henan, and Hebei). Population denominators were derived from China's 6th (2010) and 7th (2020) National Population Censuses, with age-specific populations estimated using averaged census data to ensure temporal comparability. Incidence rates were calculated using the age and sex composition of each PLAD. Age- and sex-specific incidence rates were computed, and sex differences were assessed using χ^2 tests. Occupational categories were consolidated into standardized groups, and proportional distributions across these groups were analyzed to identify temporal shifts in case demographics. Temporal trends in MT-ZVL incidence were evaluated using Joinpoint regression analysis to identify significant inflection points and estimate annual percent changes (APC). Future incidence rates and projected case numbers for 2025–2030 were estimated using autoregressive integrated moving average (ARIMA) models. Spatial autocorrelation was assessed at the county level using Global Moran's *I* statistic to evaluate overall clustering patterns. Standard Deviational Ellipse (SDE) analysis was applied to describe the spatial center, dispersion, and directional tendency of disease distribution. Data analysis was performed using R version 4.3.3 (R Foundation for Statistical Computing, Vienna, Austria), ArcGIS version 10.7 (Environmental Systems Research Institute, Redlands, CA, USA), and the Joinpoint Regression Program version 5.0.0 (Surveillance Research Program, National Cancer Institute, Bethesda, MD, USA).

Between 2010 and 2024, a total of 2,260 MT-ZVL cases were reported across the seven endemic provinces. The age-specific incidence demonstrated a bimodal distribution, with peak rates observed among children younger than 5 years and adults aged 60–75 years. Male predominance was statistically significant in infants <1 year ($\chi^2=4.455$, $P=0.035$) and adults aged 35–79 years (all $P<0.01$). The annual average number of cases per million population increased progressively with age after 30 years, reaching the highest levels in the 65–74-year age group, thereby identifying older adults as a primary high-risk population for MT-ZVL (Table 1). Throughout 2010–2024, MT-ZVL exhibited substantial temporal and seasonal variation. Following a steady decline from 2010 to 2014, both

incidence and case numbers increased continuously from 2015 onward, reaching 226 indigenous cases in 2024, corresponding to an incidence rate of 0.608 per 1,000,000 population. Joinpoint regression analysis revealed a clear reversal in temporal trends around 2015. MT-ZVL incidence declined significantly during 2010–2015 [APC= -15.7% , 95% confidence interval (CI): -23.6 to -10.1 , $P<0.001$], followed by a sustained and significant increase during 2015–2024 (APC= 13.1% , 95% CI: 10.0 to 17.1 , $P<0.001$). ARIMA projections indicate that without intensified control strategies, incidence will continue to rise, reaching 0.801 per 1,000,000 (95% CI: 0.081 to 1.520) by 2030, with an estimated 1,607 additional cases (95% CI: 660 to $2,554$) expected between 2025 and 2030 (Figure 1A). The geographic distribution of MT-ZVL expanded substantially during this period, with the number of counties reporting local cases increasing from 19 in 2010 to 69 in 2024, highlighting progressive transmission spread and an expanding at-risk population (Figure 1B). Seasonal analysis revealed year-round case occurrence, with a pronounced peak from March to August and the highest monthly incidence in April, accounting for over 12% of the annual total (Figure 1C). Occupational analysis (Supplementary Table S1, available at <https://weekly.chinacdc.cn/>) demonstrated that farmers and scattered children were the primary affected groups, accounting for 40.1% and 30.9% of cases, respectively. Over time, the proportion of cases among scattered children declined markedly from 42.3% in 2010 to 14.6% in 2024, whereas the proportion among farmers increased from 23.6% to 54.4% (Figure 1D).

Spatial autocorrelation analysis revealed significant clustering of MT-ZVL incidence in most years, particularly after 2020, with consistently positive Moran's *I* values (Supplementary Table S2, available at <https://weekly.chinacdc.cn/>), indicating intensifying geographic aggregation. The SDE analysis demonstrated a significant northeastward shift of the mean center from (104.86° , 33.39°) to (111.89° , 36.40°) and the area enlarged from core regions in Gansu and Sichuan to Shaanxi, Shanxi, Henan, and Hebei. Directional anisotropy peaked in 2015–2019 (Ratio= 7.32), indicating a pronounced corridor expansion, and declined in 2020–2024 (Ratio= 3.42), suggesting a transition toward areal diffusion. The consistently stable orientation (62.82° – 66.13°) reflected a persistent southwest–northeast expansion trajectory (Table 2).

TABLE 1. Sex and age characteristics of MT-ZVL in China, 2010–2024.

Age (years)	Total			Male			Female			χ^2 test	
	No. of accumulated cases	Population in endemic province (million)	Annual average number of cases per million people	No. of accumulated cases	Population in endemic province (million)	Annual average number of cases per million people	No. of accumulated cases	Population in endemic province (million)	Annual average number of cases per million people	χ^2	P
<1	103	3.48	1.98	65	1.83	2.36	38	1.64	1.54	4.455	0.0348
1–4	607	18.03	2.24	338	9.57	2.36	269	8.46	2.12	1.683	0.1945
5–9	162	22.94	0.47	84	12.24	0.46	78	10.69	0.49	0.153	0.6961
10–14	68	24.64	0.18	32	12.88	0.17	36	11.76	0.20	0.741	0.3895
15–19	63	23.04	0.18	29	12.31	0.16	34	10.74	0.21	1.377	0.2407
20–24	58	27.44	0.14	29	13.83	0.14	29	13.60	0.14	0.004	0.9485
25–29	58	25.12	0.15	33	12.65	0.17	25	12.48	0.13	1.000	0.3174
30–34	86	28.62	0.20	53	14.43	0.24	33	14.19	0.16	4.327	0.0375
35–39	104	28.20	0.25	74	14.28	0.35	30	13.92	0.14	17.532	<0.0001
40–44	87	28.05	0.21	59	14.19	0.28	28	13.86	0.13	10.328	0.0013
45–49	148	29.04	0.34	104	14.62	0.47	44	14.42	0.20	23.476	<0.0001
50–54	168	26.85	0.42	132	13.51	0.65	36	13.34	0.18	53.679	<0.0001
55–59	127	24.99	0.34	100	12.46	0.53	27	12.52	0.14	42.303	<0.0001
60–64	128	18.30	0.47	96	9.24	0.69	32	9.06	0.24	30.801	<0.0001
65–69	143	16.47	0.58	107	8.15	0.87	36	8.31	0.29	36.657	<0.0001
70–74	104	11.59	0.60	75	5.70	0.88	29	5.89	0.33	21.891	<0.0001
75–79	38	7.61	0.33	31	3.60	0.57	7	4.00	0.12	17.826	0.0000
80–84	8	4.47	0.12	6	2.01	0.20	2	2.46	0.05	2.916	0.0877

Note: Population in endemic province (million) = (Population of the corresponding age group from the 6th National Population Census in 2010 + Population of the corresponding age group from the 7th National Population Census in 2020) / 2 / 1,000,000. Annual average number of cases per million people = (Age-specific number of accumulated cases / Age-specific population in endemic province × 1,000,000) / 15.

DISCUSSION

This nationwide analysis demonstrates that the epidemiology of MT-ZVL in China has undergone a substantial transition over the past 15 years. The most notable findings include a shift in high-risk populations from scattered children to farmers and older adults, a clear reversal in incidence trends after 2015, and persistent spatial clustering with geographic expansion into previously unaffected areas. Together, these patterns reflect evolving transmission dynamics and mounting challenges for disease control. Historically, MT-ZVL in China disproportionately affected young children, likely due to peri-domestic exposure to *P. chinensis*. Our findings indicate a declining proportion of cases among scattered children and a growing burden among farmers, who now represent the primary high-risk group. This shift may be driven by sustained occupational exposure to *P.*

chinensis habitats linked to agricultural activities, livestock shelters, and rural living environments (6). The increasing incidence among older adults further suggests cumulative exposure and potential age-related susceptibility. Similar occupational risk patterns have been reported in other endemic regions globally, where rural and agricultural populations bear the highest disease burden (7). However, the underlying causes of this epidemiological shift remain unclear; further studies are therefore needed to clarify the determinants of these changes and to inform more targeted control interventions. The observed resurgence of MT-ZVL after 2015 suggests that earlier control gains have not been fully sustained (4,8). Multiple factors may contribute to this resurgence, including reduced intensity of vector and reservoir control, ecological changes, rural land-use transformation, and increased human mobility (8–9). The pronounced seasonal peak from spring to summer aligns with *P. chinensis* activity

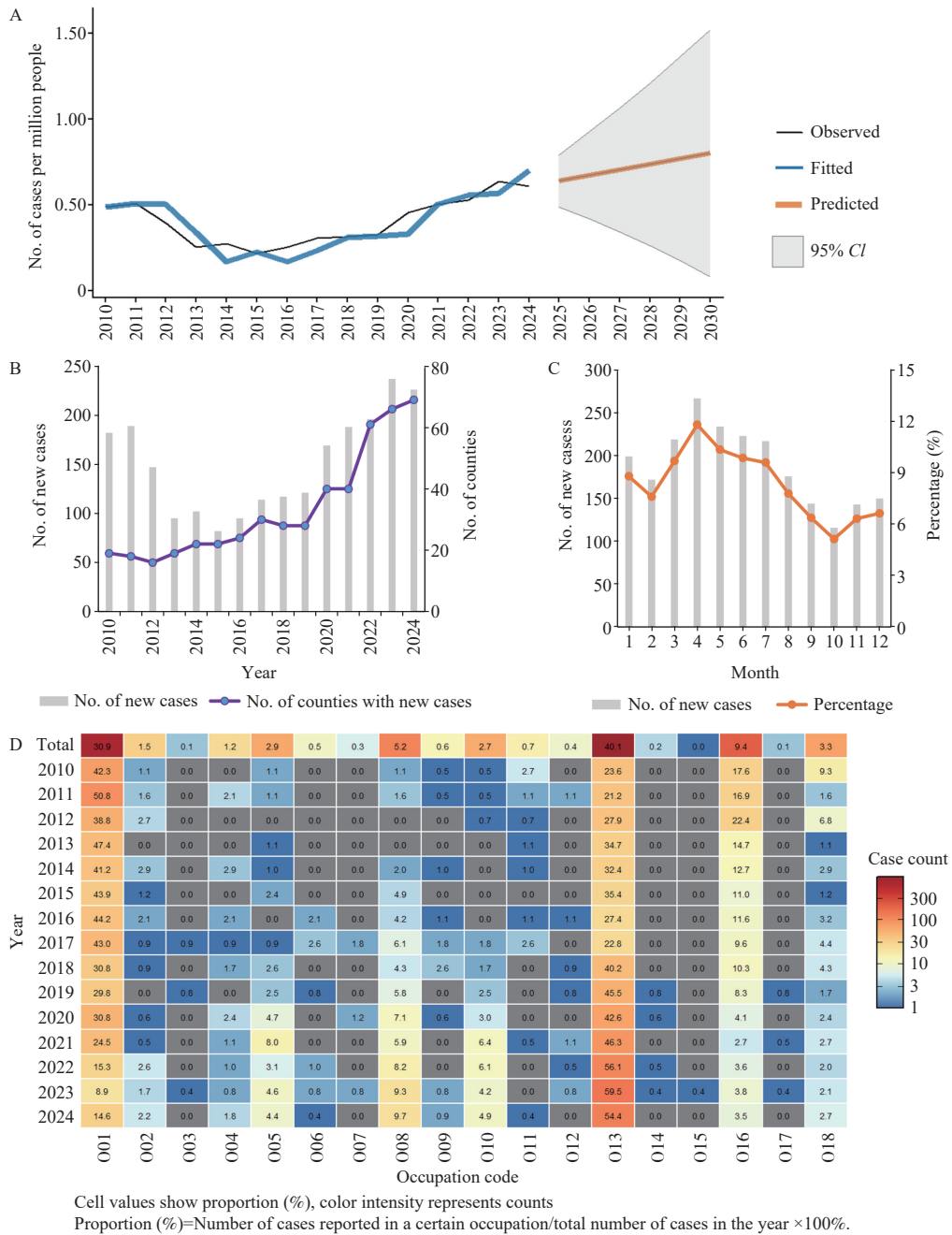


FIGURE 1. Temporal-spatial trends, seasonal patterns, and occupational distribution of MT-ZVL cases in endemic PLADs of China, 2010–2024, with incidence projections to 2030. (A) Time-trend analysis of incidence with observed, fitted, and predicted values of MT-ZVL. (B) Annual number of new indigenous cases and counties reporting cases of MT-ZVL. (C) Monthly distribution of MT-ZVL cases. (D) Heat map of the occupational distribution of MT-ZVL cases.

Note: “Observed” indicates the reported annual incidence (cases per million population) from the NNDRS; “Fitted” indicates the Joinpoint regression-based fitted trend; “Predicted” indicates the ARIMA model-based projected incidence for 2025–2030. Incidence was calculated as the number of reported cases per million population. In panel B, bars represent the number of newly reported cases, and the line represents the number of counties reporting at least one MT-ZVL case each year. In panel C, bars represent the monthly number of new cases, and the line represents the percentage of cases occurring in each month. In panel D, cell values show the proportion (%) of cases in each occupational category by year, calculated as (number of cases in a given occupation / total number of cases in that year) × 100; color intensity represents the absolute number of cases. Occupational codes (O01–O18) correspond to the standardized occupational classification used in NNDRS.

Abbreviation: MT-ZVL=mountain-type zoonotic visceral leishmaniasis; PLADs=provincial-level administrative divisions; CI=confidence interval; NNDRS=National Notifiable Diseases Reporting System.

TABLE 2. Standard deviation ellipse of distribution of MT-ZVL in China from 2010–2024.

Year	CenterX	CenterY	XStdDist	YStdDist	Rotation	Ratio
2010–2014	104.86	33.39	2.51	0.81	62.82	3.11
2015–2019	107.24	34.64	5.88	0.80	66.13	7.32
2020–2024	111.89	36.40	4.49	1.31	63.75	3.42

Note: MT-ZVL cases were grouped into three consecutive five-year periods (2010–2014, 2015–2019, and 2020–2024). The SDE was applied to characterize the spatial centrality, dispersion, and directional pattern of MT-ZVL. CenterX and CenterY denote the longitude and latitude of the mean center, indicating the overall geographic location of cases. XStdDist and YStdDist represent the standard distances along the major and minor axes of the ellipse, describing the extent of spatial dispersion in the principal expansion direction and its perpendicular direction, respectively. Rotation indicates the orientation angle (in degrees) of the major axis, reflecting the dominant direction of spatial spread. Ratio is the ratio of the major to the minor axis, representing the strength of directional anisotropy in the spatial distribution.

Abbreviation: SDE =Standard Deviation Ellipse.

and highlights the importance of timely, preseason interventions for vector control (10). Forecasting results underscore the likelihood of continued resurgence in the absence of strengthened, targeted control measures.

Spatial analyses revealed persistent clustering of MT-ZVL incidence that has intensified in recent years. Although some years exhibited weaker spatial dependence, this pattern likely reflects low overall incidence or sporadic case distribution rather than a genuine absence of clustering. The northeastward expansion indicates that MT-ZVL transmission is no longer confined to traditional endemic foci (3). These findings underscore the urgent need to extend surveillance and control efforts to newly affected areas and to allocate resources strategically based on spatiotemporal risk patterns.

Based on these findings, several public health actions are warranted. Control strategies should prioritize farmers and older adults through targeted health education, personal protective measures, and improved access to early diagnosis and treatment. Integrated approaches that combine sustained vector surveillance, dog reservoir management, and rapid response to emerging hotspots are essential to interrupt transmission cycles. This study has several limitations, including potential underreporting in surveillance data, broad occupational classifications, and the absence of analyses of environmental and socioeconomic drivers. Furthermore, the role of other reservoir hosts, such as wild animals, was not assessed and may be underestimated. Nevertheless, the extended 15-year study period and nationwide coverage provide robust evidence to inform future public health practice and policy development.

Acknowledgements: The staff at Centers for Disease Control and Prevention and Institutes of Parasitic Diseases at all administrative levels throughout China

for their invaluable assistance with data collection.

Conflicts of interest: No conflicts of interest.

Funding: Supported by the National Natural Science Foundation of China (Grant No. 82473688).

doi: 10.46234/ccdcw2026.017

Corresponding author: Shizhu Li, lisz@chinacdc.cn.

¹ National Institute of Parasitic Diseases, Chinese Center for Disease Control and Prevention; Chinese Center for Tropical Diseases Research; NHC Key Laboratory of Parasite and Vector Biology; WHO Collaborating Centre for Tropical Diseases; National Center for International Research on Tropical Diseases, Ministry of Science and Technology; National Key Laboratory of Intelligent Tracking and Forecasting for Infectious Diseases, Shanghai, China; ² School of Public Health, Fudan University, Shanghai, China; ³ Yangquan Center for Disease Control and Prevention, Yangquan City, Shanxi Province, China.

Copyright © 2026 by Chinese Center for Disease Control and Prevention. All content is distributed under a Creative Commons Attribution Non Commercial License 4.0 (CC BY-NC).

Submitted: December 26, 2025

Accepted: January 26, 2026

Issued: January 30, 2026

REFERENCES

- World Health Organization. Leishmaniasis. 2023. <https://www.who.int/news-room/fact-sheets/detail/leishmaniasis>. [2025-12-19].
- Li YY, Luo ZW, Hao YW, Zhang Y, Yang LM, Li ZQ, et al. Epidemiological features and spatial-temporal clustering of visceral leishmaniasis in mainland China from 2019 to 2021. *Front Microbiol* 2022;13:959901. <https://doi.org/10.3389/fmicb.2022.959901>.
- Hao YW, Hu XK, Gong YF, Xue JB, Zhou ZB, Li YY, et al. Spatio-temporal clustering of mountain-type zoonotic visceral leishmaniasis in China between 2015 and 2019. *PLoS Negl Trop Dis* 2021;15(3):e0009152. <https://doi.org/10.1371/journal.pntd.0009152>.
- Luo ZW, Zhou ZB, Gong YF, Feng JX, Li YY, Zhang Y, Li SZ. Current status and challenges of visceral leishmaniasis in China[J]. *Chinese Journal of Parasitology and Parasitic Diseases*, 2022, 40(2): 146-152. doi: 10.12140/j.issn.1000-7423.2022.02.003.
- Zhou ZB, Lyu S, Zhang Y, Li YY, Li SZ, Zhou XN. Visceral leishmaniasis — China, 2015-2019. *China CDC Wkly* 2020;2(33):625–8. <https://doi.org/10.46234/ccdcw2020.173>.
- Yared S, Deribe K, Gebreselassie A, Lemma W, Akililu E, Kirstein OD, et al. Risk factors of visceral leishmaniasis: a case control study in north-western Ethiopia. *Parasit Vectors* 2014;7:470. <https://doi.org/10.1186/>

- s13071-014-0470-1.
7. Geto AK, Berihun G, Berhanu L, Desye B, Daba C. Prevalence of human visceral leishmaniasis and its risk factors in eastern Africa: a systematic review and meta-analysis. *Front Public Health* 2024;12: 1488741. <https://doi.org/10.3389/fpubh.2024.1488741>.
 8. Meng Z, Fan PW, Fan ZX, Chen S, Jiang H, Shi Y, et al. Environmental change increases the transmission risk of visceral leishmaniasis in central China around the Taihang mountains. *Environ Health* 2025;24(1):27. <https://doi.org/10.1186/s12940-025-01180-9>.
 9. Zhao YZ, Jiang D, Ding FY, Hao MM, Wang Q, Chen S, et al. Recurrence and driving factors of visceral leishmaniasis in central China. *Int J Environ Res Public Health* 2021;18(18):9535. <https://doi.org/10.3390/ijerph18189535>.
 10. Zhao J, Ullah I, Fan HX, Li XH. Epidemiological insights and clinical management of paediatric kala-azar in Shanxi Province (2014-2023): retrospective analysis of case characteristics and therapeutic strategies. *BMJ Paediatr Open* 2025;9(1):e003131. <https://doi.org/10.1136/bmjpo-2024-003131>.

SUPPLEMENTARY MATERIAL

SUPPLEMENTARY TABLE S1. Occupational codes (O01–O18) correspond to the standardized occupational classification used in NNDRS.

Occupational code	Standardized occupational classification in NNDRS
O01	Scattered children
O02	Unknown
O03	Catering or food industry staff
O04	Public servant
O05	Worker
O06	Business service personnel
O07	Seafarer / Long-distance driver
O08	Household / Unemployed personnel
O09	Teacher
O10	Retiree
O11	Migrant worker
O12	Herdsman
O13	Farmer
O14	Individual business owners
O15	Soldier
O16	Students
O17	Medical worker
O18	Preschool care children

Abbreviation: NNDRS= National Notifiable Disease Reporting System.

SUPPLEMENTARY TABLE S2. Annual Moran's *I* for MT-ZVL in China, 2010–2024.

Year	Moran's <i>I</i>	Expected Moran's <i>I</i>	Variance	Z value	P
2010	0.199207	-0.055556	0.007169	3.008891	0.002622
2011	0.115745	-0.058824	0.007738	1.984564	0.047193
2012	-0.010381	-0.076923	0.008036	0.742313	0.457898
2013	0.018307	-0.055556	0.007083	0.877634	0.380143
2014	0.462370	-0.047619	0.017123	3.897345	0.000097
2015	0.239765	-0.047619	0.011142	2.722587	0.006477
2016	0.198821	-0.043478	0.011625	2.247288	0.024622
2017	0.148021	-0.035714	0.008758	1.963371	0.049603
2018	0.217221	-0.034483	0.021843	1.703061	0.088557
2019	0.129253	-0.033333	0.034376	0.876910	0.380535
2020	0.816739	-0.025641	0.008262	9.267503	0.000000
2021	1.298336	-0.027778	0.018219	9.824665	0.000000
2022	0.446089	-0.017544	0.004211	7.144700	0.000000
2023	0.075549	-0.000345	0.000010	24.178686	0.000000
2024	0.328612	-0.014706	0.007249	4.032223	0.000055